Contents lists available at ScienceDirect

Ecological Indicators

journal homepage: www.elsevier.com/locate/ecolind

bZIPs regulate laminarin metabolism via the circadian rhythms in diatom *Phaeodactylum tricornutum*

Haodong Luo , Wanying Ma , Hao Fang , Zidong Liu , Syed Shabi Ul Hassan Kazmi , Yanmei Fan , Zhen Wang , Xiaojuan Liu [*]

Guangdong Provincial Key Laboratory of Marine Disaster Prediction and Prevention, Guangdong Provincial Key Laboratory of Marine Biotechnology, Institute of Marine Sciences, STU-UNIVPM Joint Algal Research Center, College of Sciences, Shantou University, Shantou 515063, Guangdong, China

ABSTRACT

The basic region/leucine zipper motif (bZIP) transcription factor (TF) family is one of the most important gene families in plants, regulating the plant growth, development, reproduction, as well as stress responses. It was well known that some bZIP TFs in higher plants can regulate polysaccharide metabolism. However, bZIP TFs in microalgae and their function on the polysaccharide metabolism are still unknown. In this study, bioinformatic and molecular methods were carried out to analyze bZIP TFs in the diatom *Phaeodactylum tricornutum* (Pt). As a result, a total of twenty-two PtbZIP genes were identified and subsequently classified into seven distinct clades based on phylogenetic relationships, conserved motifs, and gene structures. The number of introns varied from zero to three among the PtbZIP genes. All PtbZIP genes were randomly distributed to 16 chromosomes, and each containing one or two PtbZIP domains. Among the 22 identified PtbZIP genes, PtbZIP12 and PtbZIP13 genes were identified as a putative pair of duplicated genes. Furthermore, it was observed that laminarin content increased during the day and decreased during the night. It was proposed that the 12 PtbZIPs showing the same circadian rhythms could positively affect the accumulation of laminarin, while the 10 PtbZIP genes with the opposite expression pattern might have a negative effect on the laminarin metabolism. Based on these findings, a regulatory mechanism for laminarin biosynthesis was proposed in *P. tricornutum*. The results of this study provide valuable information for further analysis of bZIP TFs functions and laminarin metabolism in microalgae, which may be useful for optimizing the mass production of laminarin.

1. Introduction

Diatoms are the main primary producers and play an important role in the carbon cycle of the earth (Yang et al., 2020). They fix carbon dioxide to synthesize bio-macromolecular polysaccharide laminarin (Alderkamp et al., 2007). Laminarin has different biological activities, such as immunomodulation, regulation of blood lipid and glucose, anti-oxidation, anti-radiation, anti-cancer, and anti-tumor effects (Huang et al., 2021). Therefore, laminarin has been widely used in food, cosmetic and medical industries. The metabolic pathway of laminarin in diatom, such as in *Phaeodactylum tricornutum*, was proposed in our recent publication (Chen et al., 2021). However, the regulatory mechanism of laminarin metabolism remains unclear.

Transcription factors (TFs) are important in the regulation of gene expression and affect the accumulation of compounds, such as carbohydrates, protein, and lipid. Among all the different transcription factors, basic leucine zipper (bZIP) transcription factors, which are widely found in eukaryotic cells, regulate important biochemical and physiological processes in plants and other eukaryotic organisms (Sornaraj et al., 2016). The bZIP domain contains two regions: one region is encoded by about 16 amino acid residues, containing a nuclear localization signal followed by an invariant N-x7-R/K motif, while the other region is a heptad repeat of leucine or bulky hydrophobic amino acids positioned exactly-nine amino acids towards to the C-terminus, creating an amphipathic helix. The bZIP can bind to DNA via the interaction between the hydrophobic sides of their helices and create a superimposing coiled-coil structure.

The bZIP TFs have different functions in different kingdoms. In animals, bZIP TFs are related with immune response (Aichmüller et al., 2020). In viruses, some bZIP TFs are key viral gene for pathogenesis (Matsuoka and Mesnard, 2020). In fungi, bZIP TFs are involved in the biosynthesis of bioactive compounds, oxidative stress response and the

---

processes of cellular morphologic change (Wang et al., 2020). At the same time, bZIP TFs in fungi are involved in the regulation of host manipulation (Figueroa et al., 2021). Furthermore, transcription factors play essential roles in plant growth and development, activating component syntheses (such as the synthesis of carbohydrates) and responses to environment changes (Wu and Gallagher, 2012). For example, it has been reported that bZIP TFs play an important role in the response of plants to parasitical fungi (Shin et al., 2020). In *Arabidopsis thaliana*, bZIPs are divided into ten groups, and each group has its specific functions depending on different domains (Jakoby et al., 2002). Group A, C, D, G, I, and S of bZIP TFs have important functions in plant growth. Group A is related to adaptability of plants under abiotic stresses depending on ABA signal (Banerjee and Roychoudhury 2017; Joo et al., 2021), such as in ginseng (Li et al., 2021), Arabidopsis (Yao et al., 2020), and soybean (Yang et al., 2020). The interaction of group C and Prolamin box binding factor protein (PBF) regulates seed storage protein. Group G is associated with ultraviolet and blue light signal transduction to regulate the synthesis of plant active molecules (Hao et al., 2019). Group I is related to the regulation of vascular development. Group S is the largest group in bZIP TFs, relating to the balance of carbohydrate demand and supply (Jakoby et al., 2002), and the expression of Group S is regulated by sucrose signal and environmental stress (Matiolli et al., 2011).

However, the functions of bZIP in microalgae have not been well studied. Depending on the phylogenetic analysis of bZIP TFs, it has been inferred that bZIP TFs in algae and angiosperm might have similar functions, as they share the same ancestry (Peviani et al., 2016). In higher plants, bZIP network serves as the energy regulatory center (Dröge-Laser and Weiste, 2018) and can be regulated by sugar signals (Matiolli et al., 2011). It's involved in sugar metabolism, protein networking, and DNA binding (Kang et al., 2010). Therefore, it is necessary to study if bZIP TFs regulate the metabolism of laminarin in microalgae, such as in diatom *P. tricornutum*. The amount of laminarin exhibits diurnal variation (Jallet et al., 2016). And bZIP TFs also have circadian expression in higher plants (Ufaz et al., 2011). It's already known that the biosynthesis of some compounds, such as sugar in tomato (Sagor et al., 2016), artemisinin in *Artemisia annua* (Hao et al., 2019), terpene in *A. thaliana* (Michael et al., 2020) and camptothecin in *Camptotheca acuminata* (Chang et al., 2019), dependents on light. Hence, it's speculated that the diurnal varied bZIP TFs might be related to the accumulation of these compounds (e.g., laminarin).

In this study, the model diatom *P. tricornutum* was used to study the bZIP TFs. Bioinformatic and molecular biological methods were employed to analyze the gene structures, phylogenetic relationships, chromosomal localization, and expression patterns of bZIP TFs. The insights gained from this investigation will provide crucial information for further functional research of bZIPs. Additionally, the findings of this study will have significant implications for mass production of laminarin in diatoms, which can be used widely in food, medicine, and medical industries.

2. Materials and methods

2.1. P. tricornutum bZIP sequence retrieval and analysis

The *P. tricornutum*'s protein sequence date (Phaeodactylum_tricornutum.ASM15095v2.pep.all.fa), DNA sequence data (Phaeodactylum_tricornutum.ASM15095v2.dna.toplevel.fa), mRNA sequence data (Phaeodactylum_tricornutum.ASM15095v2.cds.all.fa) and gene annotation data (Phaeodactylum_tricornutum.ASM15095v2.51.gff3) were available at the Ensembl Genomes (https://ensemblgenomes.org/). The Hidden Markov Model (HMM) was used to identify *P. tricornutum* bZIP candidates, and the HMM profile of bZIP (PF00170) was downloaded from the Pfam (https://pfam-legacy.xfam.org/) protein database. HMMER software (Johnson et al., 2010) was used to search against the P. tricornutum protein sequence using default parameters.

Subsequently, the remaining sequences were checked for the conserved bZIP domains using SMART (https://smart.embl.de/), Pfam, and CDD (https://www.ncbi.nlm.nih.gov/Structure/bwrpsb/bwrpsb.cgi). Finally, sequences with complete bZIP domains were selected and named based on their chromosomal locations.

2.2. Gene structure and conserved motif characterization

The protein sequences of *P. tricornutum* bZIP were uploaded to ExPASy (https://web.expasy.org/protparam/) to calculate the number of amino acids, molecular weights, and isoelectric points. Conserved motifs were predicted using the MEME program with parameters set to any number of repetitions, an optimum motif width of 10–200 residues, and searching for 10 motifs, with all other parameters set to default. The predicted motif sequences were annotated by SMART (SMART: Main page (embl.de)), CDD (Home - Conserved Domains - NCBI (nih.gov)), and Pfam (Pfam is now hosted by InterPro (xfam.org)). Additionally, the Gene Structure Display Server (Hu et al., 2015) was used to display the exon–intron structures of *P. tricornutum* bZIP genes.

2.3. Chromosomal location and gene duplication

The chromosome position of bZIP genes were retrieved from Ensembl Genomes and analyzed using Docker. The mapping of bZIP gene was analyzed using Map Chart software (Gu et al., 2002). Two genes located in the same chromosomal fragment (less than 100 kb) and separated by five or fewer genes were identified as tandem duplicated genes (Wang et al., 2010). The duplicated *P. tricornutum* bZIP gene segments were confirmed by searching the Plant Genome Duplication Database (Lee et al., 2013).

2.4. Phylogenetic analysis and classification

The phylogenetic tree was constructed using full-length amino acid sequences of bZIP from P. tricornutum. MEGA7 was used to generate an unrooted Neighbor-joining phylogenetic tree with the following parameters: 1,000 times bootstrap test, Poisson model and pairwise deletions. The classification of *P. tricornutum* bZIP proteins was based on the topology and bootstrap values of the phylogenetic tree (Tamura et al., 2007).

2.5. Microalgae material, growth conditions

P. tricornutum cells were cultured in a temperature controlled incubator in the laboratory. The microalgae were grown in f/2 medium at pH 7.6–7.8 and maintained in an artificial climate chamber with a photoperiod of 12 h light/12 h dark at 20 ± 1 ℃. The microalgal cells were collected every 4 h during a 24-hour cycle. All samples were immediately frozen in liquid nitrogen and stored at −80 ℃.

2.6. Gene expression date and analysis

The expression data of genes were measured by Beijing Genomics Institute. The gene expression levels were analyzed at seven time points, including 0, 4, 8, 12, 16, 20, and 24 h. The expression levels at 0 h were used as the control. The expression profiles of bZIP genes were plotted using Origin software. Hierarchical cluster analysis was carried out via heat mapper (https://www.heatmapper.ca/expression/). RNA sequencing (RNA-seq) was used to investigate the transcriptional responses of PtbZIPs. DEGs were determined by DEseq2. Genes with an adjusted $P < 0.05$ and $|Log2 (Fold Change)| > 1$ were considered as DEGs and the Venn diagrams were constructed using the TBtools.

3. Results

3.1. Identification and characterization of PtbZIPs in P. tricornutum

Overall, 27 putative PtbZIP transcription factors were identified by HMMER. The complete PtbZIP domains were further verified using SMART, CDD and Pfam. As a result, 22 PtbZIP proteins were confirmed in *P. tricornutum*. These PtbZIP proteins were named from PtbZIP1 to PtbZIP22 (Table 1). The length of PtbZIP proteins ranged from 165 (PtbZIP12) to 867 (PtbZIP6) amino acids. The conserved PtbZIP domain was found to contain 61 amino acids. The molecular weights of the proteins varied from 18.1 kDa (PtbZIP12) to 93.4 kDa (PtbZIP6). The 22 PtbZIP genes were randomly distributed to 16 chromosomes. The iso-electric point values of PtbZIP proteins ranged from 4.87 (PtbZIP11) to 9.81 (PtbZIP4). Except PtbZIP4, PtbZIP8, PtbZIP9, PtbZIP16 and PtbZIP18-20, all other PtbZIP proteins were predicted to be located to nucleus (Table 1).

3.2. Gene structure and motif analysis of PtbZIPs

Gene organization plays a vital role in the evolution of multiple gene families. A Neighbor-joining phylogenetic tree of PtbZIPs was constructed using MEGA7 (Fig. 1A). The MEME program was used to identify the conserved motifs of PtbZIPs and the predicted motifs were annotated. Ten conserved motifs were identified and varying in length from 8 to 100 residues (Fig. 1B). Details of the 10 motifs were listed in Table 2. Each PtbZIP protein contained a different number of conserved motifs, ranging from one to five. PtbZIP17, PtbZIP5, PhbZIP8, PtbZIP15, PtbZIP19 and PtbZIP4 had only one conserved motif, while PtbZIP21, PtbZIP6, PtbZIP14 and PtbZIP1 contained 5 conserved motifs. It was observed that PtbZIPs in the same individual clade shared the same or similar motif structures. For example, PtbZIP18, PtbZIP20 and PtbZIP9 contained two motifs, motif 1 and 2. Except motif 3 in PtbZIP3/12/13, motif 1 was the first motif on PtbZIPs. The genomic sequence and corresponding cDNA sequence of PtbZIPs were submitted to GSDS to show their gene structures. The number of introns varied from zero to three (Fig. 1C). Among them, 7 (30.4 %) genes did not have intron, while 9 (39.1 %) genes contained one intron. The remaining genes had two or three introns.

3.3. Phylogenetic analysis of the bZIP protein family

The evolutionary relationship of the PtbZIPs was analyzed by aligning the protein sequences of 22 PtbZIPs via ClustalX 1.83. The phylogenetic tree was constructed by MEGA7. The 22 PtbZIP proteins were classified into 3 distinct clades based on their evolutionary relationships, named group 1 to group 3 (Fig. 2). Group 1 consisted of 8 PtbZIP genes in an independent clade, while group 2 harbored 3 PtbZIP genes with high bootstrap value. However, group 3 was the largest group, composed of 11 PtbZIPs.
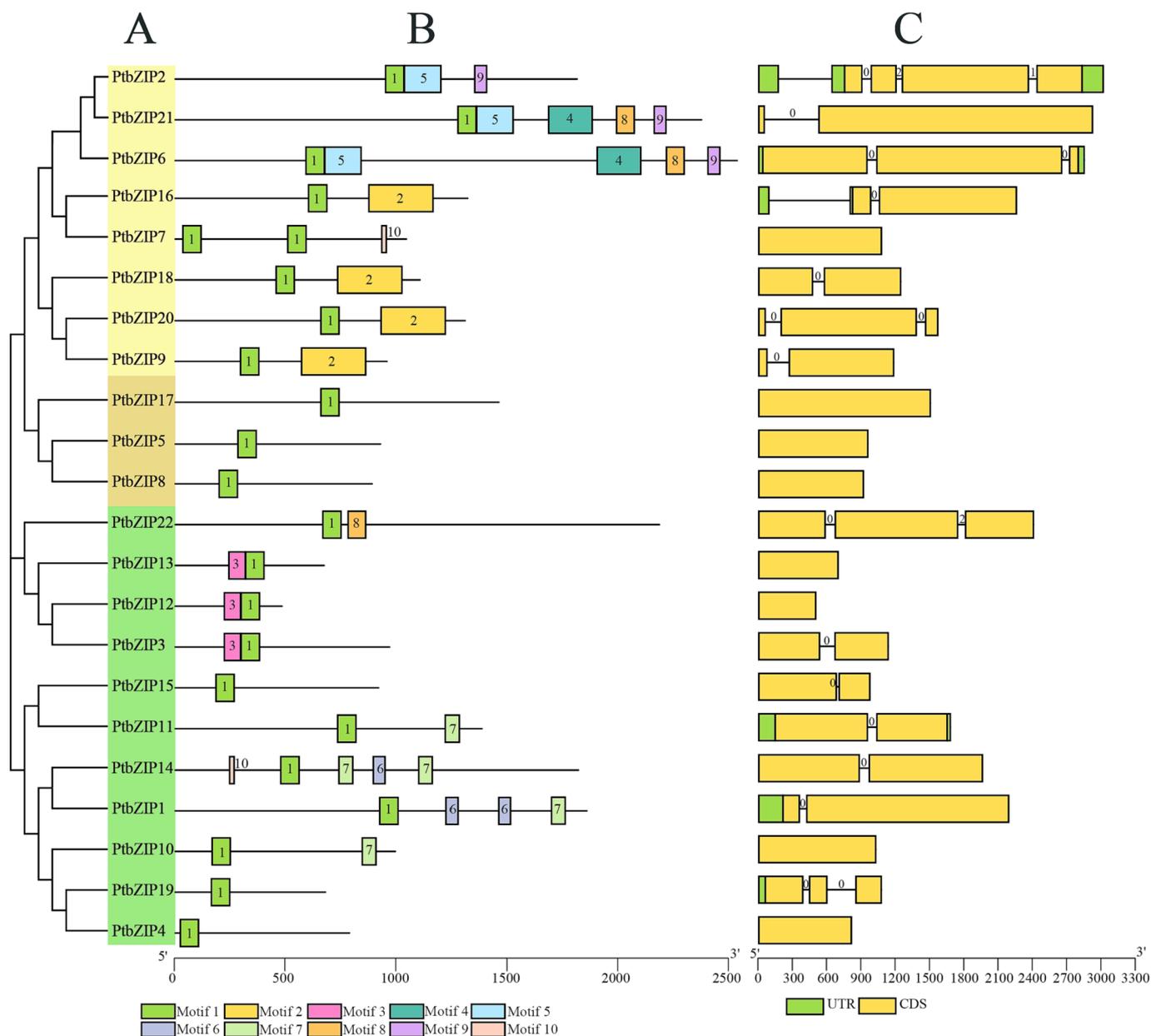
3.4. Chromosomal location and gene duplication

The distribution of PtbZIP genes was uneven on chromosomes (Fig. 3). Only 16 of 33 chromosomes had PtbZIP genes and the number of PtbZIP genes on each chromosome varied from one to two. Most of PtbZIP genes were located on the proximate or the distal ends of *P. tricornutum* chromosomes. The detailed chromosomal locations of PtbZIP genes were shown in Table S1.

Gene duplication events occur during the process of evolution (Kent et al. 2003; Mehan et al., 2004), and the expansion of gene families and genomic evolution mechanisms were mainly dependent on gene duplication events (Vision et al., 2000). In PtbZIP genes, two tandem duplicated genes, PtbZIP12 and PtbZIP13, were observed on chromosome 13 (Fig. 3). Segmental duplication was also analyzed for the PtbZIP genes. Although 7 pairs of P. tricornutum genes were tandem duplicated, PtbZIP genes were not included.

3.5. The PtbZIP expression pattern during the 24 h photoperiod

To demonstrate the expression pattern of PtbZIP genes during the 24-hour photoperiod, the differentially expressed genes of P. tricornutum were measured by BGI (Beijing Genomics Institute), and the expression of PtbZIP genes was extracted from this data. The details of PtbZIP genes' expression in 12 h light/12 h dark were shown in Supplementary Table 3. A heatmap of all PtbZIP expression was generated (Fig. 4). Based on the expression pattern, PtbZIP genes were divided into two groups. One group had high expression under the light but low expression under the dark, while the other group had opposite pattern. In the heatmap, PtbZIP4, 20, 12, 18, 13, 22, 1, 7, 17, 21, 16 and 15 were included in the first group, while PtbZIP11, 10, 6, 8, 19, 2, 9, 14, 5 and 3 were contained in the second group. Although some genes were up or

Table 1
The bioinformatic characteristics of PtbZIPs.

gene ID	gene Name	number of amino acids	molecular weight (kDa)	isoelectric point	subcellular localization
Phatr3_J42560	PtbZIP1	635	70.31	8.1	Nucleus
Phatr3_J42577	PtbZIP2	620	66.6	5.28	Nucleus
Phatr3_J43303	PtbZIP3	331	36.4	5.4	Nucleus
Phatr3_J43744	PtbZIP4	269	28.7	9.81	extra-cell, Nucleus
Phatr3_J44700	PtbZIP5	317	33.85	6.24	Nucleus
Phatr3_J45142	PtbZIP6	867	93.4	6.03	Nucleus
Phatr3_EG02108	PtbZIP7	357	40.11	8.89	Nucleus
Phatr3_J45409	PtbZIP8	304	32.08	6.29	ER, Nucleus
Phatr3_J51933	PtbZIP9	327	35.79	5.04	ER, Nucleus
Phatr3_EG00991	PtbZIP10	340	38.08	5.4	Nucleus
Phatr3_J46173	PtbZIP11	473	51.18	4.87	Nucleus
Phatr3_J47278	PtbZIP12	165	18.1	6.03	Nucleus
Phatr3_J47279	PtbZIP13	230	25.68	7.81	Nucleus
Phatr3_J47686	PtbZIP14	622	68.32	8.84	Nucleus
Phatr3_J47944	PtbZIP15	314	35.01	6.57	Nucleus
Phatr3_J15468	PtbZIP16	451	48.84	4.92	ER, Nucleus
Phatr3_J49099	PtbZIP17	499	54.16	9.39	Nucleus
Phatr3_J8113	PtbZIP18	378	41.5	5.26	ER, Nucleus
Phatr3_J49205	PtbZIP19	232	24.7	5.3	ER, Nucleus
Phatr3_J15977	PtbZIP20	447	48.79	5.83	ER, Nucleus
Phatr3_J50039	PtbZIP21	812	89.3	6.4	Nucleus
Phatr3_EG00162	PtbZIP22	747	80.77	8.69	Nucleus

Fig. 1. Gene structure, phylogenetic relationship, and conserved motifs of PtbZIPs. (A) Phylogenetic tree of 22 PtbZIPs. An unrooted Neighbor-joining phylogenetic tree of 22 PtbZIPs was constructed using the full-length amino acid sequences of proteins via MEGA7 software. (B) Conserved motifs of the PtbZIP proteins. Ten predicted conserved motifs of PtbZIP proteins represented by different colored boxes, with motif indicated by the scale at the bottom of the figure. Further details of each motif were presented in Table 2. (C) Exon-intron organization of PtbZIP genes. Yellow boxes represent exon. Black lines between two yellow boxes represent introns. Blue boxes indicate the upstream and downstream regions of PtbZIP genes. The numbers 0, 1, and 2 indicate the intron position. The sizes of exons can be estimated by the scale at the bottom of the figure. CDS: coding sequence, UTR: untranslated regions.

downregulated during the same photoperiod, the timing of the changes was different, such as PtbZIP9 and PtbZIP10, PtbZIP7 and PtbZIP21.

Subsequently, the differential expression of PtbZIP genes in a 12 h light/ 12 h dark cycle was shown in a curve graph (Fig. 5). It was observed that the expression levels of most PtbZIP genes were lower than 2000 except PtbZIP2 and PtbZIP6. Additionally, the fluctuation range of PtbZIP gene expression, except PtbZIP2 and PtbZIP6 was between 0 and 2000. The expressions of PtbZIP2 and PtbZIP6 genes were significantly downregulated during the light period, especially on the first 4 h. After that, their expressions were dramatically upregulated during the night period, particularly after the 12th h. This expression pattern was opposite to the accumulation of laminarin during the 24 h.

3.6. PtbZIP genes with differentially expression during the 24 h photoperiod

Totally, nineteen PtbZIP genes were differentially expressed during the photoperiod with the upregulated genes were shown in Fig. 6. It was observed that PtbZIP9 was consistently downregulated throughout the 24 h period. On the other hand, the remaining 14 PtbZIP genes, namely PtbZIP2, 4, 5, 6, 8, 10, 11, 12, 13, 14, 18, 19, 20 and 21, were only downregulated at the specific time points. For example, PtbZIP18 gene was only downregulated at the 16th hour in *P. tricornutum*. Additionally, the expression level of PtbZIP20 was significantly increased at the 12th and 24th h in cells.

Addition to the downregulated PtbZIP genes, the upregulated PtbZIP genes were also shown in Fig. 7. The Venn diagram for the up-regulated

Table 2
Sequences of 10 conserved motifs of PtbZIPs.

Motif	Width	Moti Sequence	Annotation
1	29	[RL]ERNRE[HS]A[RKA]R[ST] RLRK[KR]XL[LIV]E[ES]L[EQ][ET] [QE]VXDL	bZIP transcription factor
2	100	F[VAM][ILV][ST]DP[SKT]L[PQ] DNPIV[FY][AV]S[QDP][GD]F[LY] [KDN]LTGY[TS][LRS][DER][QE] [VI]LGRNCRFLQG[PT][EG]T[DS] [QAP][KES][AK]V[EDN][VQR] IRK[AGN][ILV][EGST][EQT]G [ENSV]D[AMTV][ST]V[CT]L[LM] NY[KRT][AV]DGT[PT]FWN[QK] [FL]F[IV]A[AS]LRD[AS][DEGQ] [NG][NC][IV][VT]N[FHY][VI]GV [QI][CTV]	PAS domain
3	26	[KI]K[KPT]Q[AIM][RK]Y[DE]P [DEG]VPM[PST][KR][DEG][AEQ] [LA][AT][AET]WR[RK]E[AQ]R	Phage_P2_GpE (PF06528)
4	68	I[ER][AF][RY]Y[HT][IL][NV][ET] [DE][DE][AM][IV][LV][AM][EG] [DN][FQ][LM]M[AC][PR][FW] [IV][FM][RT][ST][QT][DN]AV [LQ]CGA[KL][MS]E[CV][AV] [KM][PQ]GML[CR][AC][HK]F [NS][PS][AR][HN]K[IL][IV][GS] [LV]E[LM][MV][FY]D[AV]M[AG] FM	Threonyl carbamoyl-AMP synthase, C-terminal domain
5	57	[CHV][AQS][EQ]R[DT][AET] [AEL][VD][LRS][ER][RK][RT] [CQV]A[AIV][QS][HRV][ELM] [AV]E[KMQ][HQR][NE][VT]R [FKT][EKR]V[ILV][EMR][ENS]F [LF][AKQ][LY][RG][SG][NRT] [NY]E[GKT][DNR][ERV][AER] [KLR]W[AGS][AST]IL[ED][ED] [DGS][FC][FY][LT][KC]	Myb_DNA-bind_5 Myb/SANT-like DNA-binding domain
6	19	[ARW][MH]W[PF][LA][LF][CQ] [ENY]E[AMV][FGS][FL][ST][IVY] [DG][QK]EE[KY]	—
7	22	[IVS]L[CHST][PAL][ENPTV][QP] [ARSV][SAIT][KR][FY][LQV] [LAKV]W[LSTV][ADEQT] [EHLNR][NQ][RANS][DAES] [RACV][CIMVY][HADF]	—
8	28	P[FY][LT]IV[NQ]VN[AK][EL] [FW][ET][EK][MT]TGYT[AQ][EL] E[AV][EV]GK[EV][GY]L	PAS domain Protein of unknown function (DUF2653) PAS fold Glutathione peroxidase
9	19	[LI]H[YS][DEK][CKR][DN][GR] [ADQ][DNT]F[ILM][EMN][DFY] [GLV][CV][ANS][YA][PV]L	—
10	8	HRQ[RY][HR][CH]H[HK]	DUF2749 Protein of unknown function

–: annotation was not found. The square brackets indicated all the possible amino acids at the position.

genes was different from that of the down-regulated genes. A total of seven up-regulated PtbZIP genes were identified during the photoperiod, including PtbZIP1, 4, 7, 13, 17, 21 and 22. Among these, three genes (PtbZIP1, PtbZIP7 and PtbZIP22) were up-regulated throughout photoperiod. However, PtbZIP17 was only upregulated at the 12th h of cultivation.

4. Discussion

The bioinformatic analysis revealed the presence of 23 PtbZIP genes in *P. tricornutum*. Among them, 22 PtbZIP genes were expressed except for one, namely Phatr3_draftJ1724 (PtbZIP23). Interestingly, PtbZIP23 encoded two conserved bZIP domains and shared a conserved evolutionary relationship with other genomic PtbZIP genes (PtbZIP2, PtbZIP 6

and PtbZIP 21) (Fig. 8), but it was not located on the genome chromosome of *P. tricornutum*. Therefore, it was reasonably speculated that PtbZIP23 gene might be located on the genome of chloroplast or mitochondria. The expression of PtbZIP23 might be very low, therefore, it was not observed in this study. However, the localization and potential function of PtbZIP23 require further experiments to be confirmed.

Gene duplication events were important for the expansion of gene families and genomic evolution mechanisms. For example, it has been reported that WRKY gene family in *A. thaliana* underwent abundant gene duplication events, including segment duplication and tandem duplication. These duplications maintain different functions of WRKY in plants, especially under diverse abiotic and biotic stresses (Guo et al., 2019). Our recent paper showed that MYB gene family in *P. tricornutum* did not have many duplication events as compared to those in higher plants, indicating that the extent of duplication events dependents on the species. In this study, PtbZIPs had only one tandem duplicated pair, PtbZIP12 and PtbZIP13. It's proposed that PtbZIP12 and PtbZIP13 were highly conserved and had a similar function in *P. tricornutum*. Additionally, it was found that not only in microalgae, the bZIP gene family did not have many gene duplication in higher plants. For example, bZIP gene family in *Glycyrrhiza uralensis* had few gene duplications (Han et al., 2021). It's known that bZIP TFs played an important role in stress responses, such as drought and high temperature stresses in rice (Dey et al., 2016). The few duplication events in PtbZIP genes indicated that PtbZIP had functional diversity, as one PtbZIP might have different functions to respond to diverse environments.

Among the 22 PtbZIPs, 7 PtbZIP genes did not have introns, but the remaining 15 PtbZIPs contained introns. In plants, genes with few or no introns were known to have low expression (Ren et al., 2006). However, in the case of PtbZIP genes in *P. tricornutum*, it was different. For instance, PtbZIP7 without intron had a higher expression level than PtbZIP22 with two introns. Therefore, it was speculated that the expression of genes did not rely on the number of introns. Genes with introns could be transcribed through alternative splicing to form different proteins. Hence, 15 PtbZIPs with introns might be transcribed into many different mature mRNAs and proteins that functioning differently in *P. tricornutum*. Conversely, the 7 PtbZIPs without introns could be transcribed into a sole product to have specific function in *P. tricornutum*. In higher plants like grape, genes without intron were mostly shorter than genes with intron. Similar results were also observed in *P. tricornutum*. In grape, the bZIP genes without intron were mostly located to the chloroplast and participated in photosynthesis. However, PtbZIP gene without intron were all located in the cell nucleus and might have specific effects on the transcriptional regulation of genes.

Recently, it was reported that bZIP TFs in plants had four main factions, involving in plant development, the regulation of plant secondary metabolism, abiotic signaling, and biotic and abiotic stress responses. In microalgae, some bZIP TFs had the same function as those in higher plants. For example, CrbZIP TFs were involved in oxidative stress tolerance in green microalga *Chlamydomonas reinhardtii* (Choi et al., 2022). In stramenopiles, bZIP TFs contained the same conserved domains, such as PAS (Per-Arnt-Sim) and aureochromes (blue light photoreceptors) domains, that might be important for the abiotic signaling (Rayko et al., 2010). Hence, the function of bZIP TFs was related to their conserved domains. Based on the weak evolutionary relationship of bZIP TFs between *P. tricornutum* and higher plants, this might be explained by fact that marine and land environments were largely different, and diverse bZIP TFs had adapted to different environmental stresses. A previous study showed that bZIP TFs could cooperate with other TFs to regulate the metabolism in microalgae. For example, bZIP2 could bind to BLZ8 (*C. reinhardtii* basic leucine zipper transcription factor 8) gene and regulated the concentration of CO_2 in cell to respond to oxidative stress. In *P. tricornutum*, other binding domains of transcription factors such as MYB and AMP could also cooperate with PtbZIP TFs to perform their functions. So far, the domains of PtbZIP TFs have not been verified by experiments, therefore, the exactly function of PtbZIPs in the
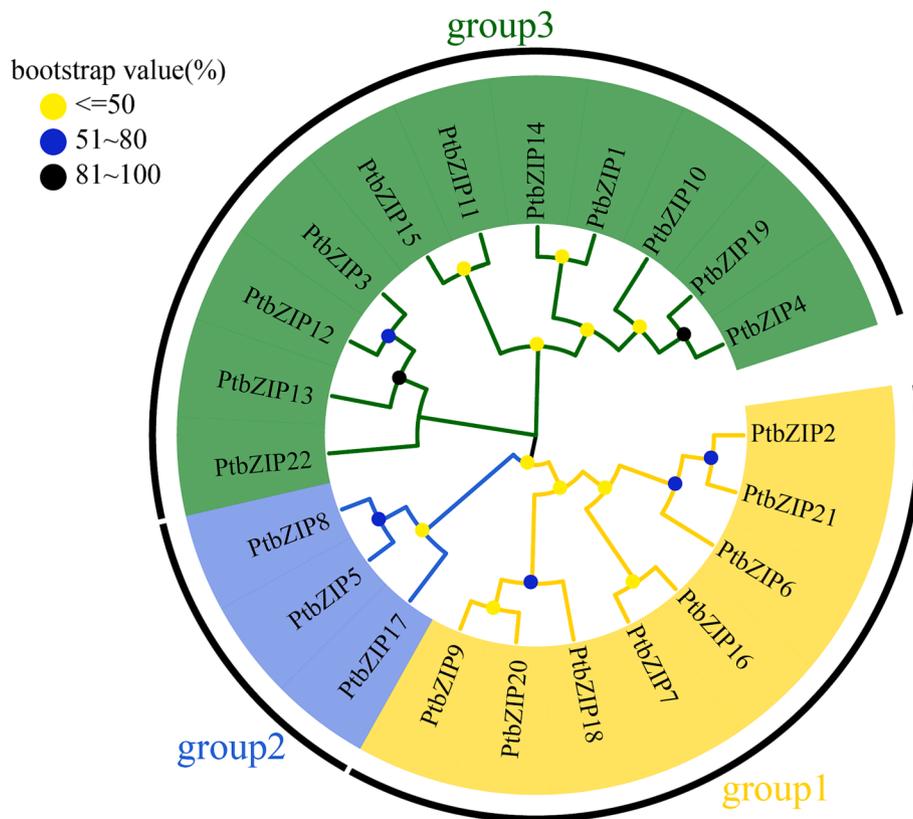
Fig. 2. Phylogenetic tree of PtbZIP proteins. The phylogenetic tree was constructed using the Neighbor-joining method with 1000 bootstrap replications. The 3 subfamilies are marked by different colors. The yellow point means the bootstrap value was lower than 50 %. The blue point means the bootstrap value ranged from 50 % to 80 %. The black point means the bootstrap value ranged from 81 % to 100 %.
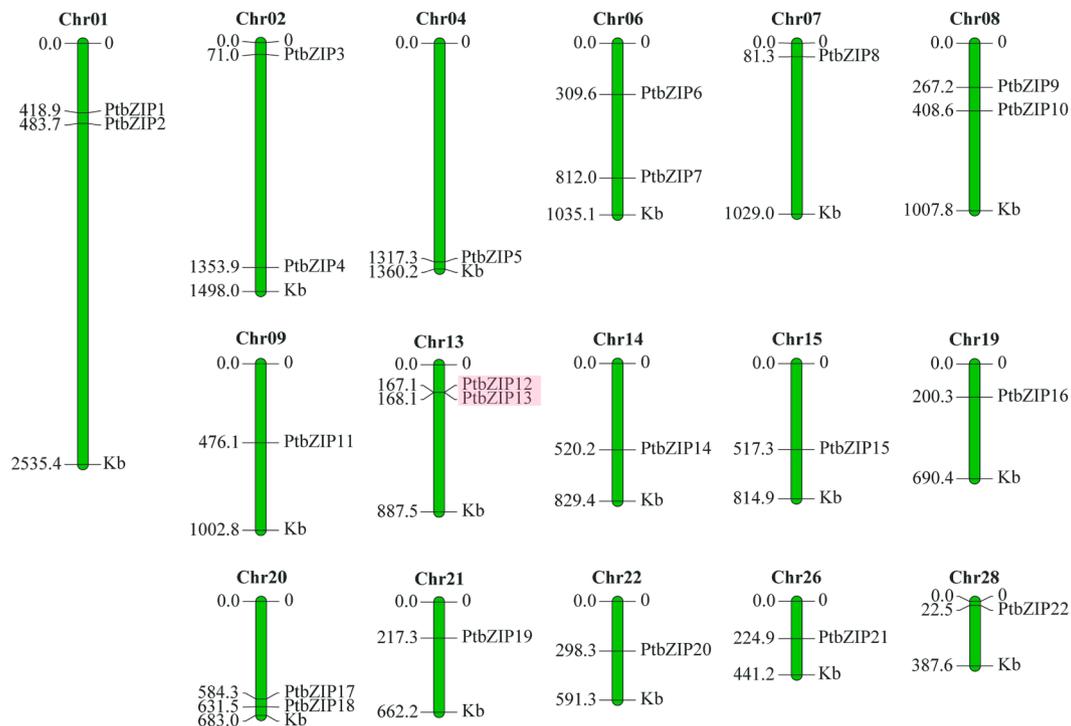
Fig. 3. The distribution of PtbZIPs on chromosomes and gene duplication. Note: Different chromosomes were shown by the green bars and the chromosome numbers were indicated above each bar. The localization of PtbZIP genes was denoted by the number (Mb) on the left side of each chromosome. The tandem duplicated genes were represented by red rectangle.
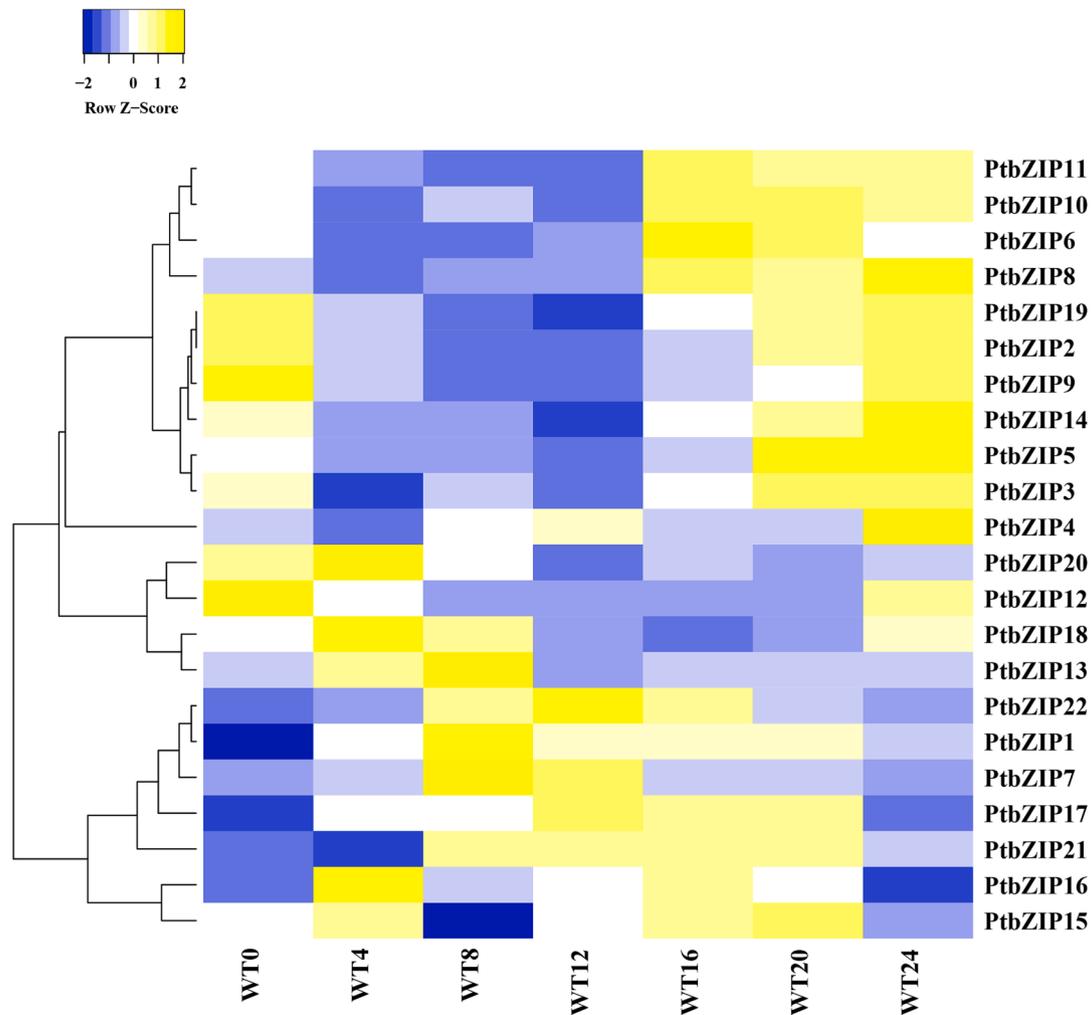
Fig. 4. Expression heatmap of PtbZIP genes in 12 h light/12 h dark. Note: WT: wild type of *P. tricornutum*. 0, 4, 8, 12, 16, 20 and 24 mean time (hour) during one photoperiod. The clustering tree was constructed by hierarchical clustering using average linkage method.
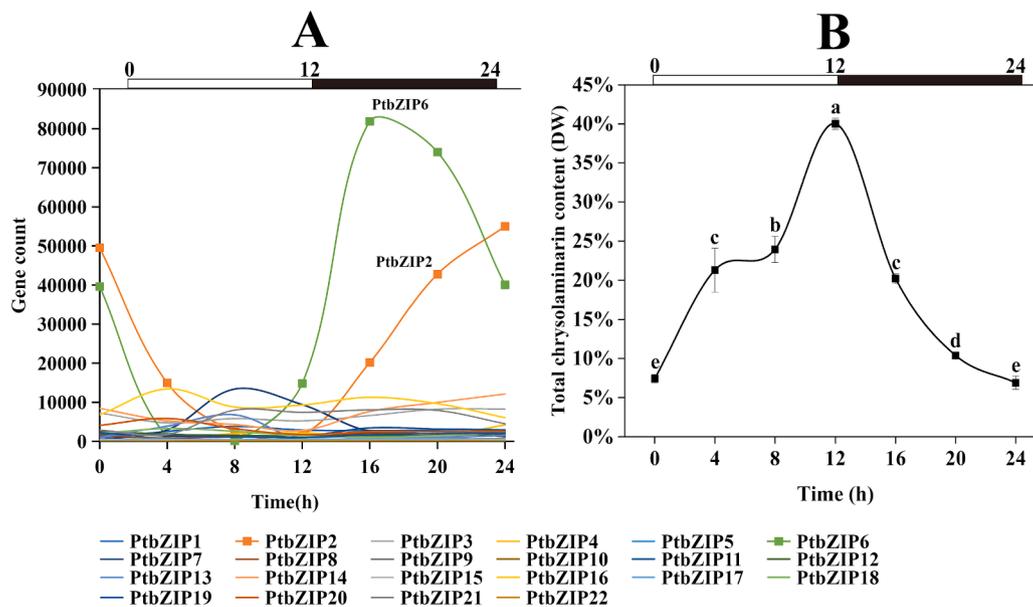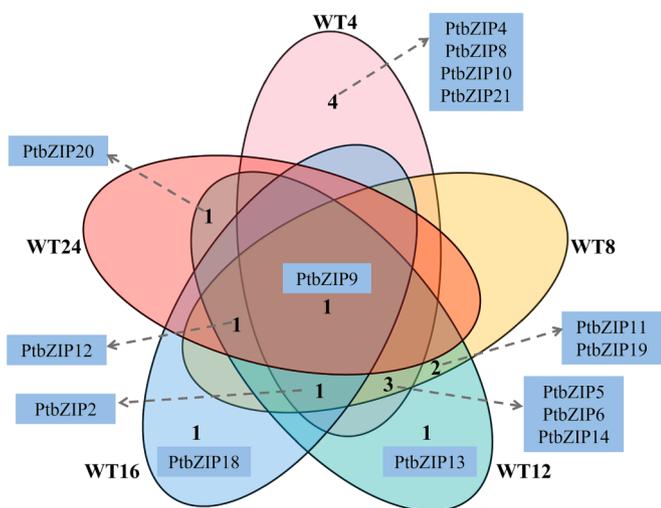

Fig. 5. PtbZIP gene expressions levels and the changes of laminarin content during the 24 h period. (A) Line graph of PtbZIP gene expression levels; (B) Changes in the content of laminarin within 24 h. The number 0, 4, 8, 12, 16, 20 and 24 were the time (h) during the 24 h period. Among them, 0, 4, 8 and12 were in the light period, while 16, 20 and 24 were in the dark period.
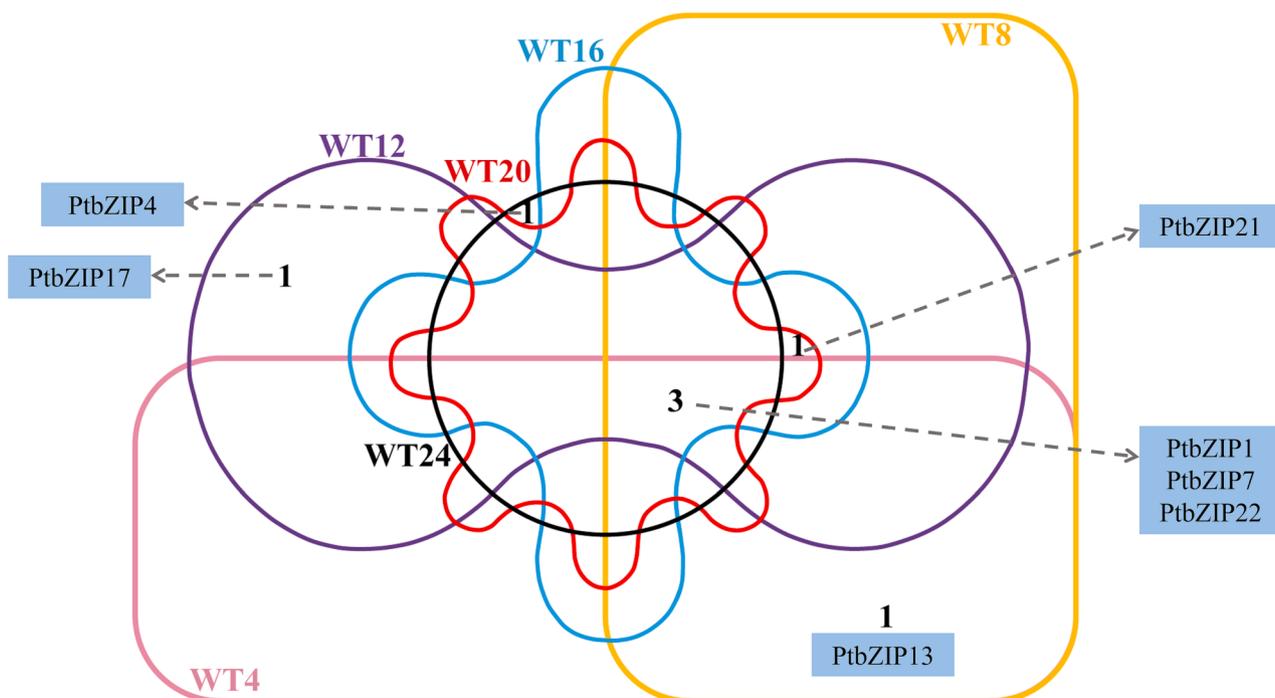
Fig. 6. Venn diagram of down-regulated PtbZIP genes. Note: The lines of different colors were different time in photoperiod. The numbers inside the lines were the number of down-regulated PtbZIP genes at that time.

regulating gene expression was still unknown.

According to the physiological analysis, it was shown that the laminarin was accumulated during the day period and degraded during the night period. This change was similar to the expression levels of PtbZIP4, 20, 12, 18, 13, 22, 1, 7, 17, 21, 16 and 15 genes, but opposite to the expression levels of PtbZIP11, 10, 6, 8, 19, 2, 9, 14, 5 and 3 genes. Aureochromes (blue light photoreceptors) domain in PtbZIP proteins could transmit light signal between day and night, so the laminarin's content might be related with PtbZIP TFs. Therefore, it was speculated that PtbZIP4, 20, 12, 18, 13, 22, 1, 7, 17, 21, 16 and 15 genes with the same circadian rhythms might have a positive effect on the regulation of laminarin accumulation, while PtbZIP11, 10, 6, 8, 19, 2, 9, 14, 5 and 3 genes might have a negative regulation on the laminarin accumulation. The specificity and affinity of bZIPs could be changed by binding to DNA

through dimerization, phosphorylation modification or interaction with other proteins, finally affecting the activation of other genes, as well as the stability and subcellular localization of bZIPs (Joo et al., 2020). bZIPs in plants usually preferentially bind to the palindromic or pseudo-palindromic *cis*-acting elements of ACGT core, such as G-box (CACGTG), c-box (GACGTC), A-box (TACGTA) and ABRE(CC-ACGTGG) (Ali et al., 2016) (E et al., 2014). In *P. tricornutum*, PtbZIP TFs might have the same characteristics as those in higher plants. Hence, the specific palindromic or pseudo-palindromic *cis*-acting elements on the promoter region of enzymes participating in the laminarin metabolism will be important binding sites for PtbZIP TFs to regulate the laminarin metabolism.

Based on the phylogenetic analysis, all 22 PtbZIPs were built into 3 individual clades. A previous study had already shown that bZIPs were involved in sugar signaling (Kang et al., 2010). Based on homology, 9 PtbZIPs might also participate in the sugar signaling. The expression pattern of all 22 PtbZIPs indicated that PtbZIP1, PtbZIP7 and PtbZIP22 which showed sustained upregulation, and PtbZIP9 which showed sustained downregulation throughout the photoperiod, might be important for the laminarin metabolism. Except for these four PtbZIP genes, the other genes showed differential expression at specific time, suggesting that they might function at specific time. For example, PtbZIP13 might play a role in the biosynthesis of laminarin during the 12th hour. However, the detailed function of these four PtbZIP genes needs further experiments to verify. It has been reported that bZIP protein was involved in DNA binding, RNA processes and protein ubiquitination (Chen et al., 2022). Together with the predicted subcellular localization of PtbZIPs, it was proposed that the nuclear PtbZIP participated in the regulation of sugar responsive genes, ultimately affecting the accumulation and degradation of laminarin (Fig. 9). Additionally, ER located PtbZIPs might be related to protein ubiquitination and participate in laminarin metabolism. Based on protein interaction prediction, the diatom response regulator (DRR) might interact with PtbZIPs (data not shown). It's known that DRR was important under light (Chen et al., 2010), therefore, it's speculated that bZIPs regulate laminarin metabolism via circadian rhythms in *P. tricornutum*.

Fig. 7. Venn diagram of up-regulated PtbZIP genes. Note: The lines of different colors were different time in photoperiod. The numbers inside the lines were the number of up-regulated PtbZIPs at that time.
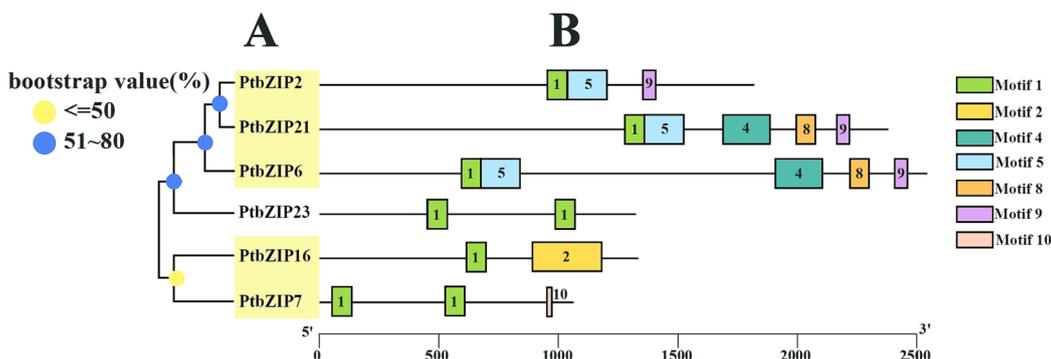
Fig. 8. The evolutionary relationship of PtbZIP23 gene and conserved motifs. Note: motif 1 was the conserved motif specific for bZIP TFs.
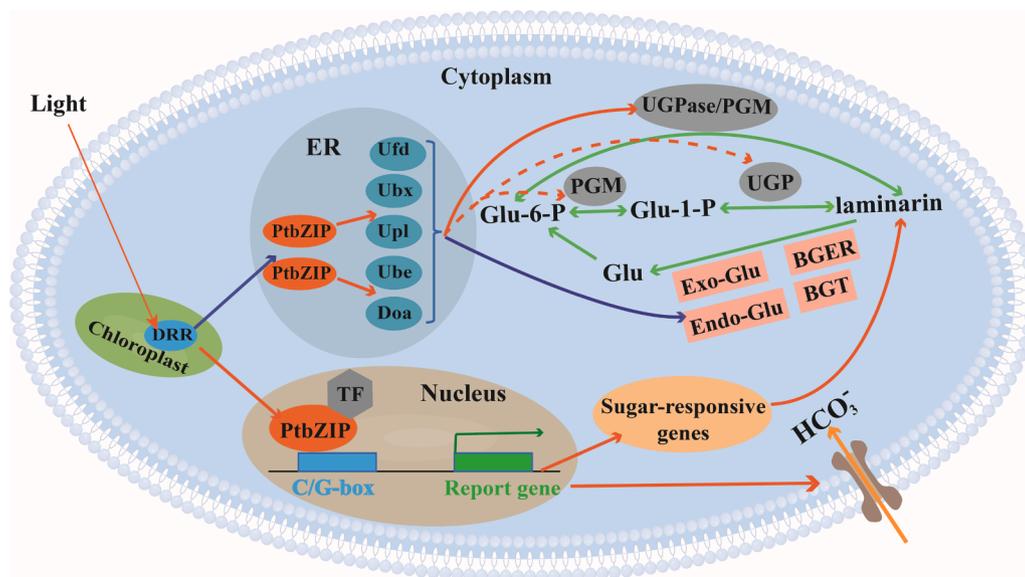

Fig. 9. Proposed mechanism of PtbZIPs on the diurnal variation of laminarin. Note: DRR, Diatom response regulator; Ufd, ubiquitin regulatory X domain-containing protein; Ubx, ubiquitin fusion degradation protein; Upl, ubiquitin-protein ligase; Ube, ubiquitin-protein ligase E3; Doa, putative degradation of alpha-2 protein; UGPase/PGM, fusion enzyme of UGP and PGM; PGM, phosphoglucomutase; UGP, UDP-glucose pyrophosphorylase; BGER, beta-glucan elicitor receptor; BGT, β-glucose transporter exo-Glu, *exo*-β-1,3-glucosidase; endo-Glu, *endo*-β-1,3-glucosidase. TF, other translation factors. Red line means auxo-action. Blue line means inhibiting effect.

5. Conclusions

Totally, twenty-two PtbZIP genes were identified from the genome of diatom *P. tricornutum*. All PtbZIP proteins were classified into 3 individual clades, named from group 1 to group 3. Most PtbZIP protein in their own group shared similar structure characteristics, including motifs, intron–exon and evolutionary relationship. PtbZIP genes were distributed to 20 chromosomes of *P. tricornutum*. PtbZIP12 and PtbZIP 13 might be duplicated genes. Laminarin was accumulated during the light period and degraded during the night period. The 12 PtbZIPs with the increasing expression during the light period and decreasing expression during the night period might positively affect the accumulation of laminarin. However, the other 10 PtbZIPs with opposite expression pattern might have a negative effect on the laminarin content. A regulatory mechanism of laminarin accumulation was proposed in P. tricornutum. The interaction of diatom response regulator (DRR) and PtbZIPs indicated that PtbZIPs might regulate laminarin metabolism via the circadian rhythms. Protein ubiquitination and sugar response genes might also be important for the biosynthesis of laminarin in *P. tricornutum*.

CRediT authorship contribution statement

Haodong Luo: Investigation, Methodology, Writing – original draft, Writing – review & editing. **Wanying Ma:** Investigation, Methodology, Writing – original draft, Writing – review & editing. **Hao Fang:** Investigation, Methodology, Writing – review & editing. **Zidong Liu:** Investigation, Methodology, Writing – review & editing. **Syed Shabi Ul Hassan Kazmi:** Writing – review & editing. **Yanmei Fan:** Writing – review & editing. **Zhen Wang:** Funding acquisition, Writing – review & editing. **Xiaojuan Liu:** Conceptualization, Project administration, Supervision, Funding acquisition, Writing – review & editing.

Declaration of Competing Interest

Data availability

Data will be made available on request.

Acknowledgements

Appendix A. Supplementary data

Supplementary data to this article can be found online at https://doi.org/10.1016/j.ecolind.2023.110210.

References

Aichmüller, C.F., Iskar, M., Jones, D.T.W., Korshunov, A., Radlwimmer, B., Kool, M., Ernst, A., Pfister, S.M., Lichter, P., Zapatka, M., 2020. Pilocytic astrocytoma demethylation and transcriptional landscapes link bZIP transcription factors to immune response. Neuro. Oncol. 22, 1327–1338. https://doi.org/10.1093/neuonc/noaa035.

Alderkamp, A.C., Van Rijssel, M., Bolhuis, H., 2007. Characterization of marine bacteria and the activity of their enzyme systems involved in degradation of the algal storage glucan laminarin. FEMS Microbiol. Ecol. 59, 108–117. https://doi.org/10.1111/j.1574-6941.2006.00219.x.

Ali, Z., Sarwat, S., Karim, I., Faridi, R., Jaskani, M., Khan, A., 2016. Functions of plant's bZIP transcription factors. Pakistan J. Agric. Sci. 53, 303–314. 10.21162/PAKJAS/16.2043.

Banerjee, A., Roychoudhury, A., 2017. Abscisic-acid-dependent basic leucine zipper (bZIP) transcription factors in plant abiotic stress. Protoplasma 254, 3–16. https://doi.org/10.1007/s00709-015-0920-4.

Chang, C., Liu, Z., Wang, Y., Tang, Z., Yu, F., 2019. A bZIP transcription factor, CaLMF, mediated light-regulated camptothecin biosynthesis in *Camptotheca acuminata*. Tree Physiol. 39, 372–380. https://doi.org/10.1093/treephys/tpy106.

Chen, C.-H., DeMay, B.S., Gladfelter, A.S., Dunlap, J.C., Loros, J.J., 2010. Physical interaction between VIVID and white collar complex regulates photoadaptation in Neurospora. Proc. Natl. Acad. Sci. U. S. A. 107, 16715–16720. https://doi.org/10.1073/pnas.1011190107.

Chen, J., Yang, J., Du, H., Aslam, M., Wang, W., Chen, W., Li, T., Liu, Z., Liu, X., 2021. Laminarin, a major polysaccharide in stramenopiles. Mar. Drugs 19, 1–11. https://doi.org/10.3390/md19100576.

Chen, J., Du, H., Liu, X., Li, T., Du, H., Wang, W., Aslam, M., Chen, W., Li, P., Luo, H., Fang, H., Liu, X., 2022. Endoplasmic reticulum-quality control pathway and endoplasmic reticulum-associated degradation mechanism regulate the N-glycoproteins and N-glycan structures in the diatom *Phaeodactylum tricornutum*. Microb. Cell Fact. 21, 1–11. https://doi.org/10.1186/s12934-022-01941-y.

Choi, B.Y., Kim, H., Shim, D., Jang, S., Yamaoka, Y., Shin, S., Yamano, T., Kajikawa, M., Jin, E., Fukuzawa, H., Lee, Y., 2022. The Chlamydomonas bZIP transcription factor BLZ8 confers oxidative stress tolerance by inducing the carbon-concentrating mechanism. Plant Cell 34, 910–926. https://doi.org/10.1093/plcell/koab293.

Dey, A., Samanta, M.K., Gayen, S., Sen, S.K., Maiti, M.K., 2016. Enhanced gene expression rather than natural polymorphism in coding sequence of the OsbZIP23 determines drought tolerance and yield improvement in rice genotypes. PLoS One 11, e0150763. https://doi.org/10.1371/journal.pone.0150763.

Dröge-Laser, W., Weiste, C., 2018. The C/S(1) bZIP network: A regulatory hub orchestrating plant energy homeostasis. Trends Plant Sci. 23, 422–433. https://doi.org/10.1016/j.tplants.2018.02.003.

Figueroa, M., Ortiz, D., Henningsen, E.C., 2021. Tactics of host manipulation by intracellular effectors from plant pathogenic fungi. Curr. Opin. Plant Biol. 62, 102054. https://doi.org/10.1016/j.pbi.2021.102054.

Gu, Z., Cavalcanti, A., Chen, F.C., Bouman, P., Li, W.H., 2002. Extent of gene duplication in the genomes of Drosophila, nematode, and yeast. Mol. Biol. Evol. 19, 256–262. https://doi.org/10.1093/oxfordjournals.molbev.a004079.

Guo, H., Zhang, Y., Wang, Z., Lin, L., Cui, M., Long, Y., Xing, Z., 2019. Genome-wide identification of WRKY transcription factors in the asteranae. Plants 8, 1–19. https://doi.org/10.3390/plants8100393.

Han, Y., Hou, Z., He, Q., Zhang, X., Yan, K., Han, R., Liang, Z., 2021. Genome-wide characterization and expression analysis of bZIP gene family under abiotic stress in *Glycyrrhiza uralensis*. Front. Genet. 12, 1–17. https://doi.org/10.3389/fgene.2021.754237.

Hao, X., Zhong, Y., Ni Tzmann, H.-W., Fu, X., Yan, T., Shen, Q., Chen, M., Ma, Y., Zhao, J., Osbourn, A., Li, L., Tang, K., 2019. Light-induced artemisinin biosynthesis is regulated by the bZIP transcription Factor AaHY5 in *Artemisia annua*. Plant Cell Physiol. 60, 1747–1760. https://doi.org/10.1093/pcp/pcz084.

Hu, B., Jin, J., Guo, A.-Y., Zhang, H., Luo, J., Gao, G., 2015. GSDS 2.0: an upgraded gene feature visualization server. Bioinformatics 31, 1296–1297. https://doi.org/10.1093/bioinformatics/btu817.

Huang, Y., Jiang, H., Mao, X., Ci, F., 2021. Laminarin and laminarin oligosaccharides originating from brown algae: preparation, biological activities, and potential applications. J. Ocean Univ. China 20, 641–653. https://doi.org/10.1007/s11802-021-4584-8.

Jakoby, M., Weisshaar, B., Dröge-Laser, W., Vicente-Carbajosa, J., Tiedemann, J., Kroj, T., Parcy, F., 2002. bZIP transcription factors in Arabidopsis. Trends Plant Sci. 7, 106–111. https://doi.org/10.1016/S1360-1385(01)02223-3.

Jallet, D., Caballero, M.A., Gallina, A., Youngblood, M.T., Peers, G., 2016. Photosynthetic physiology and biomass partitioning in the model diatom *Phaeodactylum tricornutum* grown in a sinusoidal light regime. Algal Res. Biofuels Bioprod. 18, 51–60.

Johnson, L.S., Eddy, S.R., Portugaly, E., 2010. Johnson, L.S.; Eddy, S.R.; Portugaly, E. Hidden Markov model speed heuristic and iterative HMM search procedure. BMC Bioinform. 2010, 11, 431. BMC Bioinformatics 11, 431. 10.1186/1471-2105-11-431.

Joo, H., Baek, W., Lim, C.W., Lee, S.C., 2020. Post-translational modifications of bZIP transcription factors in abscisic acid signaling and drought responses. Curr. Genomics 22, 4–15. https://doi.org/10.2174/1389202921999201130112116.

Joo, H., Baek, W., Lim, C.W., Lee, S.C., 2021. Post-translational modifications of bZIP transcription factors in abscisic acid signaling and drought responses. Curr. Genomics 22, 4–15. https://doi.org/10.2174/1389202921999201130112116.

Kang, S.G., Price, J., Lin, P.-C., Hong, J.C., Jang, J.-C., 2010. The arabidopsis bZIP1 transcription factor is involved in sugar signaling, protein networking, and DNA binding. Mol. Plant 3, 361–373. https://doi.org/10.1093/mp/ssp115.

Kent, W.J., Baertsch, R., Hinrichs, A., Miller, W., Haussler, D., 2003. Evolution's cauldron: Duplication, deletion, and rearrangement in the mouse and human genomes. Proc. Natl. Acad. Sci. 100, 11484–11489. https://doi.org/10.1073/pnas.1932072100.

Lee, T.-H., Tang, H., Wang, X., Paterson, A.H., 2013. PGDD: a database of gene and genome duplication in plants. Nucleic Acids Res. 41, D1152–D1158. https://doi.org/10.1093/nar/gks1104.

Li, H., Chen, J., Zhao, Q., Han, Y., Li, L., Sun, C., Wang, K., Wang, Y., Zhao, M., Chen, P., Lei, J., Wang, Y., Zhang, M., 2021. Basic leucine zipper (bZIP) transcription factor genes and their responses to drought stress in ginseng, Panax ginseng C.A. Meyer. BMC Genomics 22, 1–12. https://doi.org/10.1186/s12864-021-07624-z.

Matiolli, C.C., Tomaz, J.P., Duarte, G.T., Prado, F.M., Del Bem, L.E.V., Silveira, A.B., Gauer, L., Corrêa, L.G.G., Drumond, R.D., Viana, A.J.C., Di Mascio, P., Meyer, C., Vincentz, M., 2011. The Arabidopsis bZIP gene AtbZIP63 is a sensitive integrator of transient abscisic acid and glucose signals. Plant Physiol. 157, 692–705. https://doi.org/10.1104/pp.111.181743.

Matsuoka, M., Mesnard, J.-M., 2020. HTLV-1 bZIP factor: the key viral gene for pathogenesis. Retrovirology 17, 1–8. https://doi.org/10.1186/s12977-020-0511-0.

Mehan, M.R., Freimer, N.B., Ophoff, R.A., 2004. A genome-wide survey of segmental duplications that mediate common human genetic variation of chromosomal architecture. Hum. Genomics 1, 335. https://doi.org/10.1186/1479-7364-1-5-335.

Michael, R., Ranjan, A., Kumar, R.S., Pathak, P.K., Trivedi, P.K., 2020. Light-regulated expression of terpene synthase gene, AtTPS03, is controlled by the bZIP transcription factor, HY5, in *Arabidopsis thaliana*. Biochem. Biophys. Res. Commun. 529, 437–443. https://doi.org/10.1016/j.bbrc.2020.05.222.

Peviani, A., Lastdrager, J., Hanson, J., Snel, B., 2016. The phylogeny of C/S1 bZIP transcription factors reveals a shared algal ancestry and the pre-angiosperm translational regulation of S1 transcripts. Sci. Rep. 6, 30444. https://doi.org/10.1038/srep30444.

Rayko, E., Maumus, F., Maheswari, U., Jabbari, K., Bowler, C., 2010. Transcription factor families inferred from genome sequences of photosynthetic stramenopiles. New Phytol. 188, 52–66. https://doi.org/10.1111/j.1469-8137.2010.03371.x.

Ren, X.-Y., Vorst, O., Fiers, M.W.E.J., Stiekema, W.J., Nap, J.-P., 2006. In plants, highly expressed genes are the least compact. Trends Genet. 22, 528–532. https://doi.org/10.1016/j.tig.2006.08.008.

Sagor, G.H.M., Berberich, T., Tanaka, S., Nishiyama, M., Kanayama, Y., Kojima, S., Muramoto, K., Kusano, T., 2016. A novel strategy to produce sweeter tomato fruits with high sugar contents by fruit-specific expression of a single bZIP transcription factor gene. Plant Biotechnol. J. 14, 1116–1126. https://doi.org/10.1111/pbi.12480.

Shin, J., Bui, D.C., Kim, S., Jung, S.Y., Nam, H.J., Lim, J.Y., Choi, G.J., Lee, Y.W., Kim, J. E., Son, H., 2020. The novel bZIP transcription Fpo1 negatively regulates perithecial development by modulating carbon metabolism in the ascomycete fungus *Fusarium graminearum*. Environ. Microbiol. 22, 2596–2612. https://doi.org/10.1111/1462-2920.14960.

Sornaraj, P., Luang, S., Lopato, S., Hrmova, M., 2016. Basic leucine zipper (bZIP) transcription factors involved in abiotic stresses: A molecular model of a wheat bZIP factor and implications of its structure in function. Biochim. Biophys. Acta - Gen. Subj. 1860, 46–56. https://doi.org/10.1016/j.bbagen.2015.10.014.

Tamura, K., Dudley, J., Nei, M., Kumar, S., 2007. MEGA4: Molecular Evolutionary Genetics Analysis (MEGA) software version 4.0. Mol. Biol. Evol. 24, 1596–1599. https://doi.org/10.1093/molbev/msm092.

Ufaz, S., Shukla, V., Soloveichik, Y., Golan, Y., Breuer, F., Koncz, Z., Galili, G., Koncz, C., Zilberstein, A., 2011. Transcriptional control of aspartate kinase expression during darkness and sugar depletion in Arabidopsis: involvement of bZIP transcription factors. Planta 233, 1025–1040. https://doi.org/10.1007/s00425-011-1360-9.

Vision, T.J., Brown, D.G., Tanksley, S.D., 2000. The origins of genomic duplications in Arabidopsis. Science (80-.) 290, 2114–2117. https://doi.org/10.1126/science.290.5499.2114.

Wang, L., Guo, K., Li, Y., Tu, Y., Hu, H., Wang, B., Cui, X., Peng, L., 2010. Expression profiling and integrative analysis of the CESA/CSL superfamily in rice. BMC Plant Biol. 10, 282. https://doi.org/10.1186/1471-2229-10-282.

Wang, X., Zha, W., Liang, L., Fasoyin, O.E., Wu, L., Wang, S., 2020. The bZIP transcription factor AflRsmA regulates aflatoxin B1 biosynthesis, oxidative stress response and sclerotium formation in *Aspergillus flavus*. Toxins (Basel) 12, 1–17. https://doi.org/10.3390/toxins12040271.

Wu, S., Gallagher, K.L., 2012. Transcription factors on the move. Curr. Opin. Plant Biol. 15, 645–651. https://doi.org/10.1016/j.pbi.2012.09.010.

Yang, R., Wei, D., Xie, J., 2020a. Diatoms as cell factories for high-value products: chrysolaminarin, eicosapentaenoic acid, and fucoxanthin. Crit. Rev. Biotechnol. 40, 993–1009. https://doi.org/10.1080/07388551.2020.1805402.

Yang, Y., Yu, T.-F., Ma, J., Chen, J., Zhou, Y.-B., Chen, M., Ma, Y.-Z., Wei, W.-L., Xu, Z.-S., 2020b. The soybean bZIP transcription factor gene GmbZIP2 confers drought and

salt resistances in transgenic plants. Int. J. Mol. Sci. 21 https://doi.org/10.3390/ijms21020670.

Yao, L., Hao, X., Cao, H., Ding, C., Yang, Y., Wang, L., Wang, X., 2020. ABA-dependent bZIP transcription factor, CsbZIP18, from *Camellia sinensis* negatively regulates

freezing tolerance in Arabidopsis. Plant Cell Rep. 39, 553–565. https://doi.org/10.1007/s00299-020-02512-4.

E, Z.G., Zhang, Y.P., Zhou, J.H., Wang, L., 2014. Mini review roles of the bZIP gene family in rice. Genet. Mol. Res. 13, 3025–3036. 10.4238/2014.April.16.11.